Using growth and arrest of Richtmyer-Meshkov instabilities and Lagrangian simulations to study high-rate material strength

M B Prime, D E Vaughan, D L Preston, W T Buttler, S R Chen, D M Oró and C Pack

Los Alamos National Laboratory, P.O. Box 1663, Los Alamos, New Mexico, USA

E-mail: prime@lanl.gov

Abstract. Experiments applying a supported shock through mating surfaces (Atwood number = 1) with geometrical perturbations have been proposed for studying strength at strain rates up to 10^7/s using Richtmyer-Meshkov (RM) instabilities. Buttler et al. recently reported experimental results for RM instability growth in copper but with an unsupported shock applied by high explosives and the geometrical perturbations on the opposite free surface (Atwood number = -1). This novel configuration allowed detailed experimental observation of the instability growth and arrest. We present results and interpretation from numerical simulations of the Buttler RM instability experiments. Highly-resolved, two-dimensional simulations were performed using a Lagrangian hydrocode and the Preston-Tonks-Wallace (PTW) strength model. The model predictions show good agreement with the data. The numerical simulations are used to examine various assumptions previously made in an analytical model and to estimate the sensitivity of such experiments to material strength.

1. Introduction

Rayleigh-Taylor instabilities have been widely used to study the deviatoric (flow) strength of solids at high strain rates and pressures. More recently, experiments applying a supported shock through mating surfaces (Atwood number = 1) with geometrical perturbations have been proposed for studying strength at strain rates up to 10^7/s using Richtmyer-Meshkov (RM) instabilities [1, 2]. Buttler et al. recently reported experimental results for RM instability growth but with an unsupported shock applied by high explosives and the geometrical perturbations on the opposite free surface (Atwood number = -1) as shown in figure 1 [3]. Some numerical studies have used Eulerian and Molecular Dynamics simulations to study how to infer a yield strength from experimental measurements of RM instability growth and arrest [4]. In this study, we use Lagrangian simulations with advanced models of yield strength to further study the issue.

2. Experiment

The experiment, detailed elsewhere [3] uses a plane wave lens and momentum trapping target to approximate the ideal conditions illustrated in figure 1. The target uses OFHC copper in the half-hard state with a total thickness of 8 mm. The sine wave perturbations have a wavelength, λ, of 550 µm, and four initial perturbation amplitudes were studied, η_0 = 10-131 µm, to give non-dimensional $\eta_0 k$ (where $k = 2\pi/\lambda$) of 0.12, 0.35, 0.75 and 1.5. The $\eta_0 k$ = 0.35 case was the most interesting as there was

significant spike growth but then arrest. The two larger $\eta_0 k$ tests grew unstably and the smaller $\eta_0 k$ test had no significant growth. The experiments were diagnosed using proton radiography [5] and Photon Doppler Velocimetry (PDV) [6].
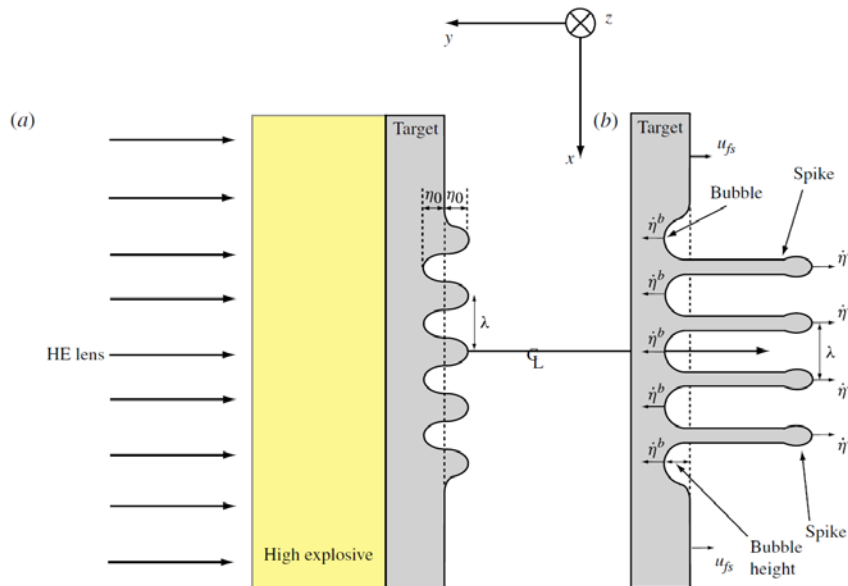

Figure 1. The pre-shock (a) and post shock (b) geometries of a Richtmyer-Meshkov instability in the A = -1 configuration. The initial perturbations invert and then grow and possibly arrest depending on the loading conditions and the properties of the target including deviatoric strength. From [3].

3. Modeling

To examine the extraction of yield strength in copper from the RMI spike heights, continuum simulations were performed using Flag, a Lagrangian hydrodynamics code [7, 8]. Each simulation used a two-dimensional plane strain mesh that modeled two full wavelengths of the perturbation, see figure 2, and had constraints on the top and bottom to prevent vertical displacements, effectively assuming periodic behavior.
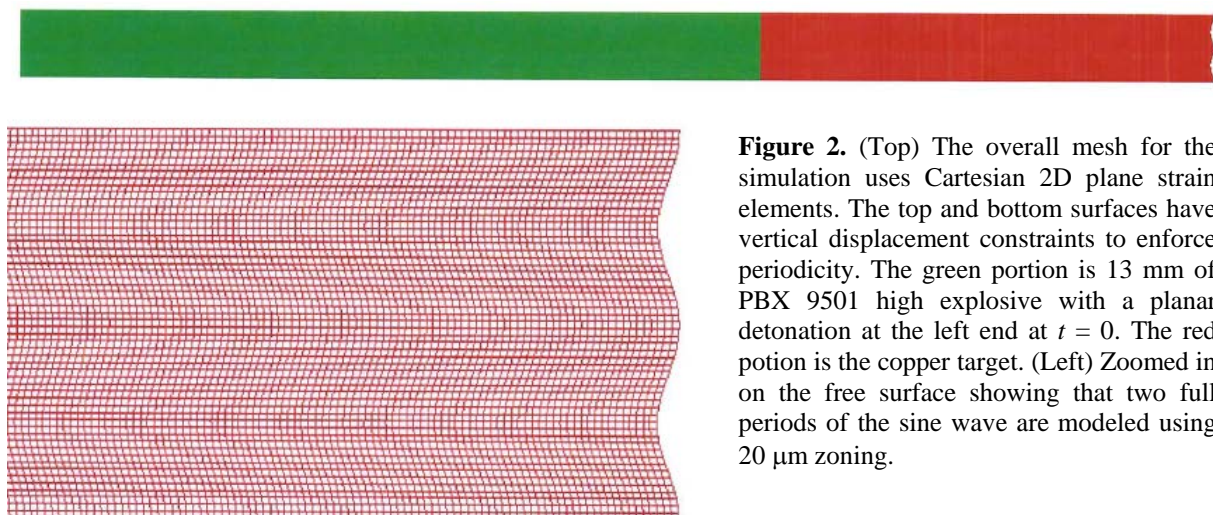

Figure 2. (Top) The overall mesh for the simulation uses Cartesian 2D plane strain elements. The top and bottom surfaces have vertical displacement constraints to enforce periodicity. The green portion is 13 mm of PBX 9501 high explosive with a planar detonation at the left end at $t = 0$. The red potion is the copper target. (Left) Zoomed in on the free surface showing that two full periods of the sine wave are modeled using 20 μm zoning.

The PBX 9501 high explosive was modeled using a tabular equation of state [9] and programmed burn. The copper impactor was modeled using SESAME tabular equation of state 3336, a Preston-Wonks-Wallace (PTW) deviatoric strength model [10], and the TEPLA damage and failure model

[11]. The PTW model was calibrated using quasi-static and Hopkinson bar stress-strain data taken at rates from 10^{-3}/s to 4300/s and temperatures from 77 K to 873 K .

4. Results

In order to check the material models prior to simulating perturbations, Figure 3 compares the model results for free surface velocity in flat regions of the target to measured free surface velocities. The quality of the match indicates that the high explosive model and the material model for copper adequately capture the loading, shock and basic spall behavior.

Figure 4 shows the simulation for $\eta_0 k = 0.35$, with the spike having undergone growth then arrest. The accumulated plastic strain reaches 65%, which is an order of magnitude less than the value reported previously [3] based on the analytical approximation [1]. The strain rate peaked at about 6×10^6/s, which is also lower than the reported average strain rate of 1.5×10^7/s. We are still investigating this discrepancy.
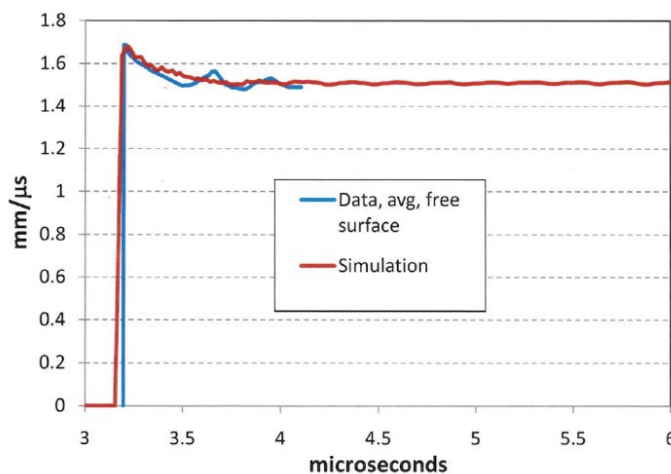

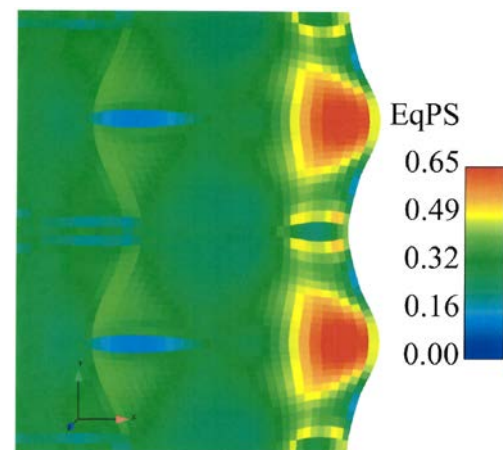**Figure 3.** The calculated free surface velocity in the flat region matches the data well.

Figure 4. Accumulated equivalent plastic strain reaches 65% after spike growth and arrest for the $\eta_0 k = 0.35$ case

Figure 5 shows that the models for the different initial perturbation sizes captured the spectrum of experimental results: from almost no growth for $\eta_0 k = 0.12$, to growth and arrest for $\eta_0 k = 0.35$, to unstable growth for $\eta_0 k = 0.75$ and 1.5. The match between velocity predictions and data are least accurate for the unstable growth case of $\eta_0 k = 1.5$. In the case of unstable growth, the spikes are expected to eventually breakup and fly ballistically. The Lagrangian calculation becomes increasingly inaccurate as the mesh deforms at higher deformations, and the calculation was not capable of simulating breakup and material separation. Thus the poorer agreement. Since the main focus was strength effects on the arrest of instabilities, no effort was made to improve the modeling for the unstable growth cases.

For $\eta_0 k = 0.35$, the model predicted a final spike growth $\eta_\infty\text{-}\eta_0$ of about 110 μm, compared to the experimentally reported value of 160 μm [3]. The difference indicates that the strength in the model was too high, and indeed the model yield strength in the spike region varied between 0.60 and 0.70 GPa, whereas the analytical approximation [1] indicated that a strength of about 0.37 GPa should match the data [3].

The overall model match to the results may appear surprisingly good considering that the estimated strain rates for the experiment (6×10^6/s) peak at more than a factor of 1000 above the highest rate data used in the PTW calibration (4×10^3/s). Two additional considerations give some confidence in the PTW model up to rates of maybe 10^5/s. First, the PTW model is validated on Taylor rod data, which achieves rates above 10^4/s. Second, the high rate Hopkinson bar data taken at 77K, which suppresses

thermally activated dislocation motion, probes the strength expected at higher rates for room temperature tests. However, somewhere above 10^5/s, phonon drag is expected to come into play, which is when the model is expected to be less accurate and is one reason why this RMI data is valuable.
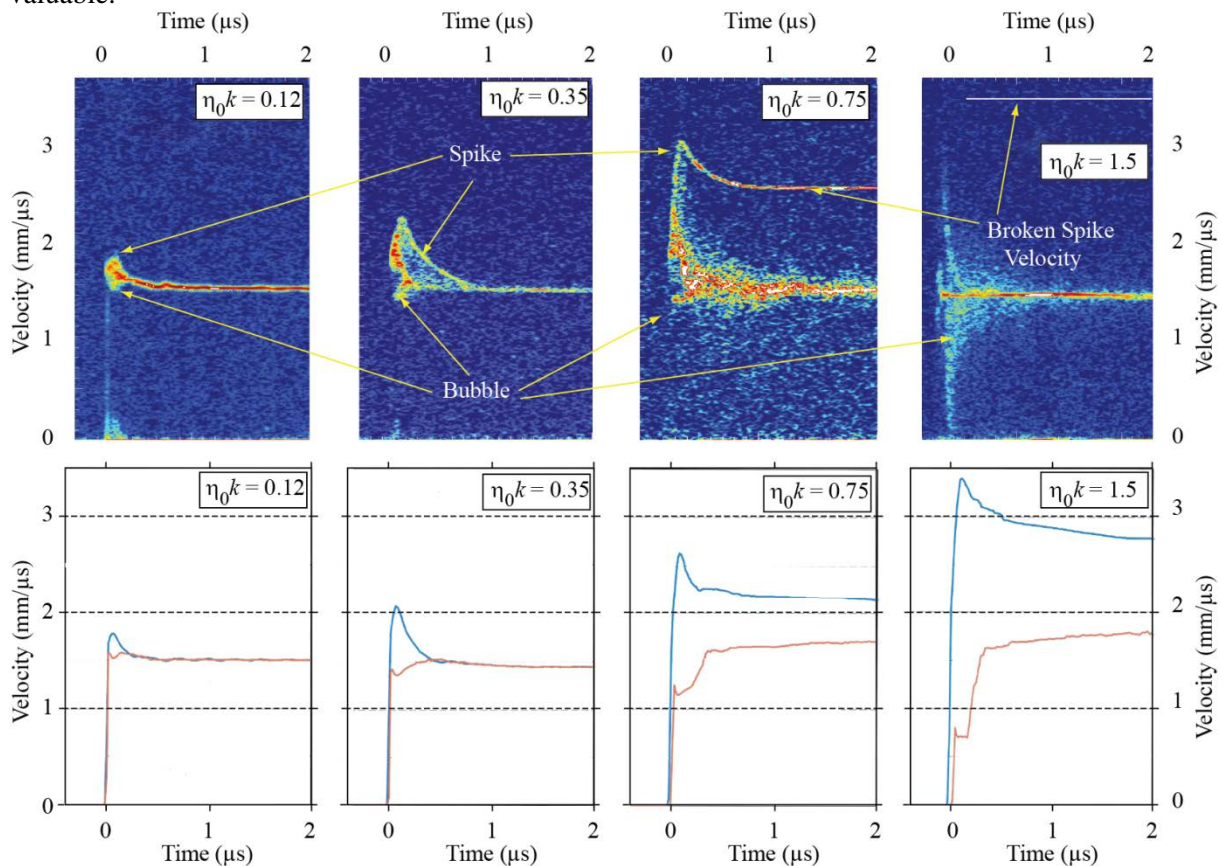

Figure 5. (Top) PDV measurements of velocities in spike and bubble regions for different $\eta_0 k$'s (from [3]) compared with model results (bottom, spike in blue and bubble in red) show the model captures the spectrum of results: from no growth, to growth and arrest, to unstable growth.

5. Deviatoric strength studies

To develop an analytical approximation for final spike height for RM instabilities, Piriz assumed single mode growth, incompressibility, a constant flow strength, and several other kinematic approximations [1]. His result was that for a given $\eta_0 k$ and shock pressure, final spike height would be inversely proportional to the flow strength Y. We simulated the $\eta_0 k = 0.35$ test using a model with a constant flow stress to examine the Piriz result. Figure 6 shows that the simulations for different values of Y matched the expected result until Y became so low that the spikes grew unstably.

In the original development of the PTW model, there were no reliable data for strain rates above 10^4/sec, and the strong shock theory was not considered valid below 10^9/sec, and so strength was effectively interpolated/extrapolated to the intermediate rates. A modification to PTW has been considered that adjusts the strength at these rates only, affecting neither the fit to data below 10^4/s nor the model in the strong shock regime [12]. Figure 7 shows the effect of the "r" parameter on the saturation stress at intermediate rates for a generic metal, where $r = 0$ is unmodified PTW. A series of calculations with different values of r were performed for copper RMI experiments with different $\eta_0 k$ to see if the RMI spike height could be used to calibrate r. Figure 8 shows the results of the study. For $\eta_0 k < 0.4$, r had a very minimal effect on the final spike height. For $\eta_0 k > 0.45$, the model predicted

spike instability no matter the r value. Only in a very narrow $\eta_0 k$ range did r have a measurable impact on the final spike height, implying that it would be difficult to calibrate r based on such measurements. The lack of sensitivity occurs because the r value adjusts the saturation stress but not the initial yield strength. Since the spikes that arrest tend to grow to modest plastic strains, less than 100%, the saturation stress does not have a large effect on the arrest. These RMI experiments would be more suited to calibrating the initial yield strength and lower-strain strength at high rates than the saturation stress.
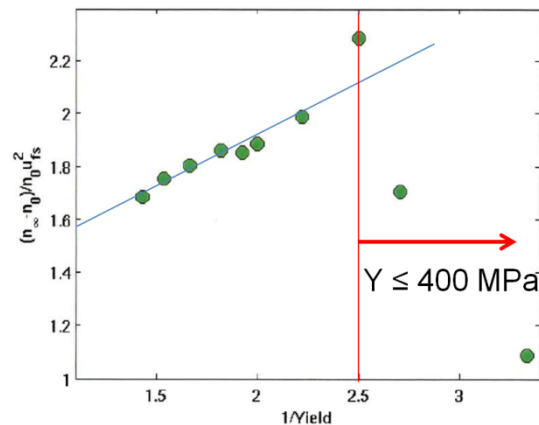

Figure 6. A set of simulations confirmed the Piriz linear relationship of final spike height with $1/Y$, until Y became so low that the spikes became more unstable.
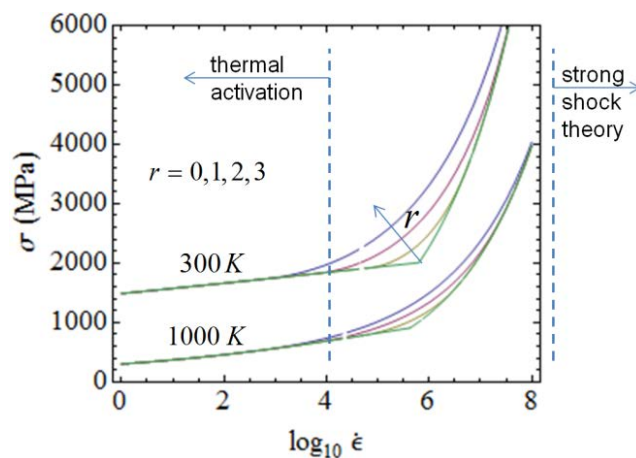

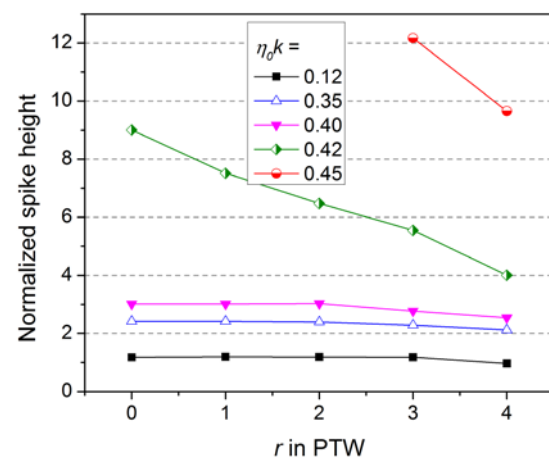**Figure 7.** The "r" value modifies the PTW strength model in the intermediate strain rate region.

Figure 8. Simulations showed that the PTW r value had only a modest impact on predicted spike height.

6. Conclusions

Richtmyer-Meshkov instabilities in the Atwood = -1 configuration have significant promise for studying deviatoric strength of solids. Such tests are relatively easy to field and diagnose, especially compared to the +1 configuration. Measureable behavior is quite sensitive to strength in $10^6 - 10^7$/s regime, which is hard to reach otherwise, and strains up to maybe 100%. However, extracting a single value for strength is difficult because of time and spatial variations of strain, strain rate, and T. Therefore, a model must be used to interpret the data. In the case of unsupported shock loading, interplay with spall/damage behavior is also an issue.

Acknowledgements

References

[1]   Piriz A R, Cela J J L, Tahir N A and Hoffmann D H H 2008 Richtmyer-Meshkov instability in elastic-plastic media *Phys. Rev.* E **78** 056401

[2]   Piriz A R, Cela J J L and Tahir N A 2009 Richtmyer–Meshkov instability as a tool for evaluating material strength under extreme conditions *Nucl. Instrum. Methods* A **606** 139-41

[3]   Buttler W T, Oró D M, Preston D L, Mikaelian K O, Cherne F J, Hixson R S, Mariam F G, Morris C, Stone J B, Terrones G and Tupa D 2012 Unstable Richtmyer-Meshkov growth of solid and liquid metals in vacuum *J. Fluid Mech.* **703** 60-84

[4]   Dimonte G, Terrones G, Cherne F J, Germann T C, Dupont V, Kadau K, Buttler W T, Oro D M, Morris C and Preston D L 2011 Use of the Richtmyer-Meshkov instability to infer yield stress at high-energy densities *Phys. Rev. Lett.* **107** 264502

[5]   King N S P, Ables E, Adams K, Alrick K R, Amann J F, Balzar S, Barnes Jr P D, Crow M L, Cushing S B and Eddleman J C 1999 An 800-MeV proton radiography facility for dynamic experiments *Nucl. Instrum. Methods* A **424** 84-91

[6]   Holtkamp D B 2006 Survey of optical velocimetry experiments-applications of PDV, a heterodyne velocimeter. In: *2006 International Conference on Megagauss Magnetic Field Generation and Related Topics,* ed G F Kiuttu*, et al.* (Santa Fe, NM: IEEE) pp 119-28

[7]   Caramana E J, Burton D E, Shashkov M J and Whalen P P 1998 The Construction of Compatible Hydrodynamics Algorithms Utilizing Conservation of Total Energy *J. Comput. Phys.* **146** 227-62

[8]   Burton D E, Carney T C, Morgan N R, Runnels S R, Sambasivan S K and Shashkov M J 2011 A cell-centered Lagrangian hydrodynamics method for multi-dimensional unstructured grids in curvilinear coordinates with solid constitutive models. *Los Alamos National Laboratory Tech. Rep.* LA-UR-11-04995

[9]   Shaw M S 2000 A theoretical equation of state for detonation products with chemical equilibrium composition of the surface of small carbon clusters *AIP Conf. Proc.* **505** 235-8

[10]   Preston D L, Tonks D L and Wallace D C 2003 Model of plastic deformation for extreme loading conditions *J. Appl. Phys.* **93** 211-20

[11]   Addessio F L and Johnson J N 1993 Rate-dependent ductile failure model *J. Appl. Phys.* **74** 1640-8

[12]   Preston D L 2010 PTW mod 1 *Los Alamos National Laboratory Tech. Rep.* LA-UR-10-06436